

# Exploring supported ionic liquids for IgY antibody purification

Amanda RP Silva,<sup>a†</sup> Catarina Almeida,<sup>b†</sup> Márcia C Neves,<sup>b</sup>  
Carlota O Rangel-Yagui<sup>a\*</sup>  and Mara G Freire<sup>b,c\*</sup> 



## Abstract

**BACKGROUND:** Immunoglobulin Y (IgY), a scalable alternative to mammalian antibodies, typically found in hen's egg yolk, has gained attraction in diagnostic and therapeutic applications. However, its purification from egg yolk remains challenging due to the complex matrix and limitations of conventional techniques. Supported Ionic Liquids (SILs), formed by covalently immobilizing Ionic Liquids (ILs) onto solid supports, offer a sustainable and tunable platform for IgY purification. Therefore, this study evaluates the potential of SILs as effective and selective adsorbent materials towards IgY, allowing its purification from the Water-Soluble Protein Fraction (WSPF) derived from hen's egg yolk.

**RESULTS:** Three SILs, namely [Ssi][C<sub>3</sub>mim]Cl, [Ssi][N<sub>3444</sub>]Cl, and [Ssi][N<sub>3888</sub>]Cl, were synthesized in a single-step process and characterized by elemental analysis, Zeta Potential measurements, Solid-state Carbon-13 Nuclear Magnetic Resonance (<sup>13</sup>C NMR), Spectroscopy and Total Reflectance-Fourier Transform Infrared Spectroscopy (ATR-FTIR). Response Surface Methodology (RSM) was applied to optimize the pH, Solid: Liquid (S:L) ratio, and contact time for the separation of IgY from the WSPF. Optimal conditions enable up to 90 and 20% IgY purity and recovery yield with [Ssi][C<sub>3</sub>mim]Cl. Alongside the achieved high purity, this approach demonstrated reduced solvent usage and operational simplicity.

**CONCLUSION:** SILs represent a promising strategy for sustainable purification of IgY antibodies. Their high tunable surface chemistry, and environmentally friendly synthesis align current demands for greener and more efficient downstream processes. To this end, this work advances the development of next generation bioseparation technologies with potential industrial applicability.

© 2026 The Author(s). *Journal of Chemical Technology and Biotechnology* published by John Wiley & Sons Ltd on behalf of Society of Chemical Industry (SCI).

Supporting information may be found in the online version of this article.

**Keywords:** immunoglobulin Y; water-soluble protein fraction; purification; supported ionic liquids; adsorption

## INTRODUCTION

Antibodies are widely regarded as the preferred affinity molecules for therapeutic, biochemical, and analytical applications.<sup>1</sup> Immunoglobulin G (IgG) is the most common member of this class, with well-established applications, for instance treatment and prevention of various infections.<sup>2</sup> However, immunoglobulin Y (IgY) represents a promising technological advancement.<sup>1</sup>

IgY, present in egg yolk, is analogous to human IgG. In 1996, the high IgY technology gained international recognition, referring to the process of producing antibodies for diagnosis, prophylaxis, and immunotherapy through the extraction, manufacturing, and application of IgY antibodies.<sup>3</sup> Over the past decade, this technology has seen significant advancements in technical aspects, as well as in clinical and scientific applications.<sup>4</sup> Some IgY-based products have entered the commercial market, attracting substantial investments from various industries to further commercialize IgY technologies.<sup>4,5</sup>

The purification of IgY from the egg yolk typically involves extracting the water-soluble protein fraction (WSPF) through a

straightforward dilution process. Common techniques for purifying IgY from the WSPF include precipitation methods that utilize salts (such as ammonium sulfate) or polymers (like polyethylene glycol), which often involve multiple steps.<sup>6</sup> Chromatographic techniques, while effective, can be costly and time-consuming.<sup>7,8</sup> Furthermore, some of these purification methods face scalability

\* Correspondence to: CO Rangel-Yagui, University of São Paulo – School of Pharmaceutical Sciences, Brazil, E-mail: [corangel@usp.br](mailto:corangel@usp.br); or MG Freire, CICECO - Aveiro Institute of Materials, Department of Chemistry, University of Aveiro, Portugal. E-mail: [maragfreire@ua.pt](mailto:maragfreire@ua.pt)

† These authors contributed equally.

a School of Pharmaceutical Sciences, University of São Paulo, São Paulo, Brazil

b CICECO - Aveiro Institute of Materials, Department of Chemistry, University of Aveiro, Aveiro, Portugal

c RYA - Purification Technologies, Ílhavo, Portugal

challenges.<sup>8</sup> Consequently, there is a pressing need to develop more cost-effective and optimized alternatives for the extraction and purification of IgY on an industrial scale. In this context, supported ionic liquids (SILs) offer a favorable and environmentally sustainable technology for protein purification.

Ionic liquids (ILs) present several advantages when employed for the capture and/or purification of target biocompounds in complex biological matrices.<sup>9,10</sup> ILs are usually described as green solvents due to their negligible volatility and non-flammable nature.<sup>11</sup> They typically consist of an organic cation and an organic or inorganic anion, exhibiting high chemical, thermal, and electrochemical stability.<sup>12,13</sup> ILs can be tailored by modifying the structures of their cations and anions to achieve desirable properties, such as enhanced selectivity and separation performance. When covalently bonded to a solid matrix, such as silica, SILs are formed. These facilitate various interactions between the functionalized solid support and the target compound, resulting in improved selectivity when processing biological matrices.<sup>10,12,13</sup>

While SILs have been successfully employed in the separation of various compounds,<sup>14–19</sup> their application in protein purification remains relatively underexplored.<sup>13,20–23</sup> This gap is particularly evident in the context of antibody purification. To the best of our knowledge, only IgG antibodies have been purified from rabbit serum and Chinese hamster ovary (CHO) cell culture supernatants using SILs.<sup>10</sup> SILs have not been investigated for the purification of other antibodies, such as IgY antibodies. In this study, three ionic liquids were employed to functionalize a spherical silica matrix and were evaluated as adsorbents for the capture/purification of IgY antibodies from the water-soluble protein fraction of egg yolk.

## MATERIALS AND METHODS

Spherical silica gel, employed as support material, with a particle size ranging from 75 to 200  $\mu\text{m}$ , acquired from Merck, was activated with and hydrochloric acid (HCl, 37 wt%) from Sigma-Aldrich. To prepare the SILs, it was used 3-chloropropyltrimethoxysilane (98% purity), *N*-methylimidazole (99% purity) and tributylamine (99% purity), acquired from Acros Organics; triethylamine (>98% purity), provided by Fluka; ethanol (99% purity) and toluene (99% purity), acquired from Fisher Scientific, and methanol (99% purity), purchased from Fisher Chemical. To prepare the WSPF from hen's egg yolk, commercial eggs, acquired from a local supermarket, were used. To evaluate the effect of pH on the adsorption of the major proteins found in WSPF, *i.e.*, IgY,  $\alpha$  and  $\beta$ -livetins, different buffer solutions were used, namely the citrate/phosphate (0.1 M citric acid/0.2 M  $\text{Na}_2\text{HPO}_4$ ) and the carbonate/bicarbonate (0.1 M  $\text{Na}_2\text{CO}_3$ /0.1 M  $\text{NaHCO}_3$ ) buffers for pH values ranging from 3.0 to 7.0 and from 9 to 11, respectively. The first one was prepared with sodium chloride (99.5% purity), anhydrous monobasic sodium phosphate (99% purity) and sodium phosphate dibasic heptahydrate (98% purity), all acquired from Thermo Scientific, and citric acid monohydrate (>99% purity), purchased from Fisher Scientific. The latter was prepared using sodium carbonate ( $\geq 99.5\%$  purity) and sodium bicarbonate (99% purity), acquired from Sigma Aldrich and Thermo Scientific, respectively. To prepare the Size-Exclusion High Performance Liquid Chromatography (SE-HPLC) mobile phase, it was used anhydrous monobasic sodium phosphate (99% purity), sodium phosphate dibasic heptahydrate (98% purity), and sodium chloride (99.5% purity), all acquired from Thermo Scientific.

## Synthesis of the supported ionic liquids (SILs)

Three SILs, with chloride as the counterion and spherical silica as a support, were synthesized, namely 1-methyl-3-propylimidazolium chloride ([Ssi][C<sub>3</sub>mim]Cl), propyltributylammonium chloride ([Ssi][N<sub>3444</sub>]Cl) and propyltriethylammonium chloride ([Ssi][N<sub>3888</sub>]Cl). The synthesis protocol was adapted from Qiu *et al.*,<sup>24</sup> and previously reported by our research group.<sup>10,18,25,26</sup> A schematic diagram outlining the synthesis protocol employed for the preparation of the SILs under study is depicted in Fig. 1.

It is important to reinforce that, in this study, the spherical silica functionalization was performed in a single step. Accordingly, this material was initially activated for 24 h with HCl (37 wt%) to increase the amount of silanol groups on its surface. Afterwards, 5 g of the activated spherical silica was suspended in 60 mL of toluene, followed by the addition of 5 mL (0.026 mol) of 3-chloropropyltrimethoxysilane and 0.035 mol of the respective cation source. Then, this suspension was kept in reflux under magnetic stirring for 24 h. Subsequently, the resulting material was filtered and washed with 100 mL of toluene, 350 mL of methanol, 300 mL of distilled water, and 150 mL of methanol, followed by dry at 60 °C for 24 h.

## Characterization of the supported ionic liquids (SILs)

### Elemental analysis

The amount of carbon (%C), hydrogen (%H) and nitrogen (%N) in the three synthesized SILs, namely [Ssi][C<sub>3</sub>mim]Cl, [Ssi][N<sub>3444</sub>]Cl and [Ssi][N<sub>3888</sub>]Cl, was determined by elemental analysis, using the TruSpec LECO-CHNS 630-200-200 analyzer. To this end, approximately 2 mg of each material were analyzed at a combustion furnace temperature of 1075 °C, and a burner temperature of 850 °C. The nitrogen content was measured using thermal conductivity, whereas carbon and hydrogen contents were determined by infrared absorption.

### Bonding amount (BA)

The bonding amount (BA) ( $\mu\text{mol m}^{-2}$ ), which corresponds to the chemical amount of IL *per* area of material, was determined for all synthesized SILs ([Ssi][C<sub>3</sub>mim]Cl, [Ssi][N<sub>3444</sub>]Cl and [Ssi][N<sub>3888</sub>]Cl). Considering a specific surface area ( $S_{\text{BET}}$ ) of 288.59  $\text{m}^2 \text{g}^{-1}$  for the spherical silica and that the imidazole ring presents two nitrogen atoms, the BA for [Ssi][C<sub>3</sub>mim]Cl was determined according to the following equation:

$$\text{BA} = \frac{\% \text{N}}{2 \times \frac{M(\text{N})}{S_{\text{BET}}}} \quad (1)$$

where %N corresponds to the weight percentage of nitrogen and  $M(\text{N})$  to the molar mass of nitrogen ( $\text{g } \mu\text{mol}^{-1}$ ).

On the other hand, for [Ssi][N<sub>3444</sub>]Cl and [Ssi][N<sub>3888</sub>]Cl, a single nitrogen atom is present for each IL moiety and, therefore, the BA was determined according to the following equation:

$$\text{BA} = \frac{\% \text{N}}{\frac{M(\text{N})}{S_{\text{BET}}}} \quad (2)$$

### Point of zero charge (PZC)

The Point of Zero Charge (PZC) of [Ssi][C<sub>3</sub>mim]Cl, [Ssi][N<sub>3444</sub>]Cl, [Ssi][N<sub>3888</sub>]Cl, and activated spherical silica were determined by electrophoretic mobility, being the zeta potential measurements recorded for suspensions of each material in distilled water at

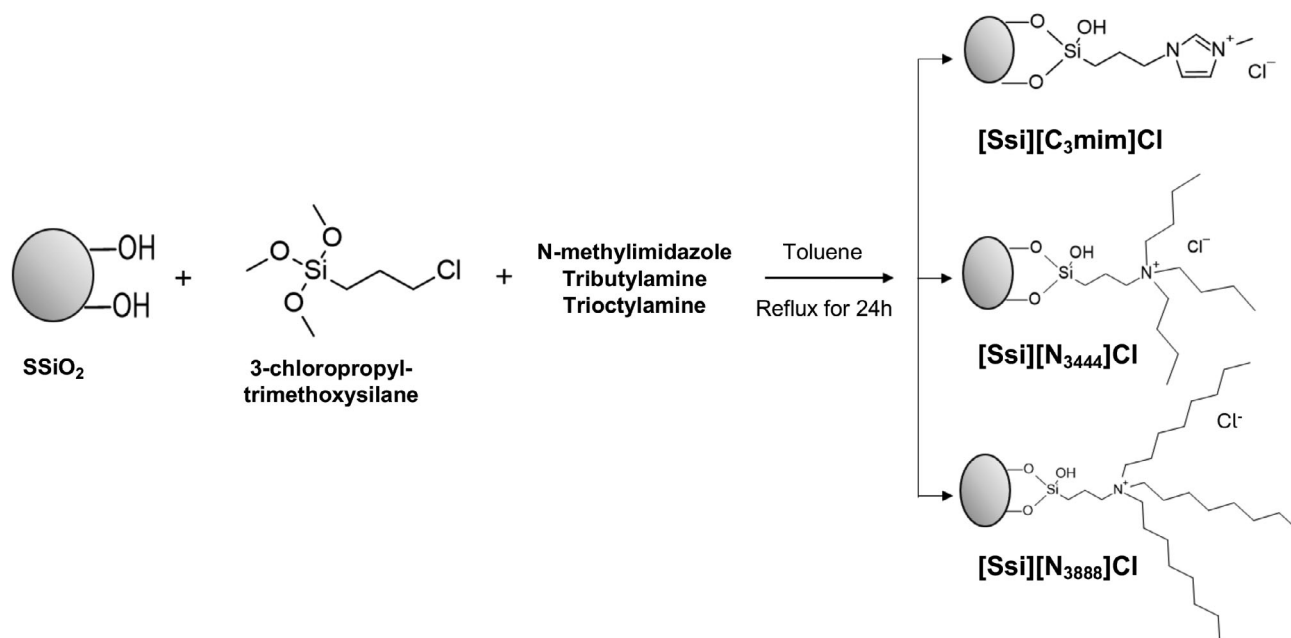


**Figure 1.** Schematic diagram outlining the synthesis protocol used to prepare the SILs in one step, accompanied by their chemical structures and respective abbreviations, *i.e.*, [Ssi][C<sub>3</sub>mim]Cl, [Ssi][N<sub>3444</sub>]Cl and [Ssi][N<sub>3888</sub>]Cl.

different pH values, which were adjusted with sodium hydroxide (NaOH) and HCl solutions of 0.1 and 0.01 M, respectively. These measurements were attained using a Malvern Zetasizer Nano ZS equipment (Malvern Instruments Ltd., Malvern, UK) and a polycarbonate folded capillary cell with gold plated copper electrodes. The following acquisition parameters were employed: minimum and a maximum of 10 and 15 runs, respectively; 3 measurements; a polystyrene latex material; water as dispersant; a temperature of 25 °C and an equilibrium time of 120 s.

#### Solid-state Carbon-13 nuclear magnetic resonance (<sup>13</sup>C NMR) spectroscopy

Solid-state carbon-13 Nuclear Magnetic Resonance (<sup>13</sup>C NMR) spectroscopy was employed to confirm the SIL synthesis ([Ssi][C<sub>3</sub>mim]Cl, [Ssi][N<sub>3444</sub>]Cl and [Ssi][N<sub>3888</sub>]Cl). Spectra were recorded on a BRUKER AVANCE III (wide-bore) spectrometer at 9.4 T, and a 4 mm double-resonance MAS probe was used at 100.6 MHz.

#### Attenuated Total reflectance- Fourier transform infrared spectroscopy (ATR-FTIR)

The activated spherical silica and the [Ssi][C<sub>3</sub>mim]Cl, [Ssi][N<sub>3444</sub>]Cl and [Ssi][N<sub>3888</sub>]Cl were chemically characterized by Attenuated Total Reflectance- Fourier Transform Infrared Spectroscopy (ATR-FTIR), using a Perkin Elmer FT-IR System Spectrum BX (Waltham, MA, USA) at 25 °C. To this end, 256 scans were performed for each sample, at a wavelength ranging from 4000 to 500 cm<sup>-1</sup>, and a resolution of 8.0 cm<sup>-1</sup>.

#### Preparation of the water-soluble protein fraction (WSPF) from the egg yolk

The WSPF was extracted from commercially acquired hen's egg yolk, according to the method described by Liu *et al.*<sup>27</sup> To this end, the egg yolk was initially separated from the egg white, followed by its 7-fold dilution with distilled water. The pH of the mixture was then adjusted to 5.0 with HCl of 1 M and frozen

overnight to facilitate a further lipid fraction separation. After thawing, the previous mixture was centrifuged for 60 min, at 4500 rpm at 4 °C. The lipid fraction (orange pellet) was discarded, and the liquid WSPF was filtered and used for the following studies.

#### Evaluation of the performance of SILs for IgY purification from WSPF

IgY was quantified in each sample through SE-HPLC.<sup>28</sup> Accordingly, the samples were diluted at a 1:2 (v:v) ratio in an aqueous potassium phosphate buffer solution (50 mmol·L<sup>-1</sup>, pH 7.0, with NaCl 0.3 mol·L<sup>-1</sup>), acting as the mobile phase. The analysis was performed on a Chromaster HPLC system (VWR Hitachi), and the apparatus included a binary pump, a Shodex Protein KW-802.5 (8 × 300 mm) column, a temperature-controlled auto-sampler (which operates at 10 °C), a column oven (which operates at 40 °C), and a DAD detector. The injection volume was 25 μL, and the mobile phase was eluted isocratically at a flow rate of 0.5 mL·min<sup>-1</sup>. Detection was carried out at a wavelength of 280 nm. The resulting chromatograms were processed, and the respective peak areas were estimated using PeakFit® software. The performance of each of the synthesized SILs ([Ssi][C<sub>3</sub>mim]Cl, [Ssi][N<sub>3444</sub>]Cl and [Ssi][N<sub>3888</sub>]Cl) for the selective adsorption, and thus purification, of IgY from WSPF was assessed by determining the percentages of its recovery yield and purity. The purity of IgY adsorbed onto the SIL was determined according to the following equation:

$$\% \text{ Purity} = \frac{A_{\text{IgY(SIL)}}}{A_{\text{total(SIL)}}} \times 100 \quad (3)$$

where,  $A_{\text{IgY(SIL)}}$  corresponds to the peak area of IgY and  $A_{\text{total(SIL)}}$  to the sum of the peak areas of all proteins adsorbed on the SIL.

The recovery yield (%) of IgY adsorbed on the SIL was determined according to the following equation:

$$\% \text{ Recovery Yield} = \frac{A_{\text{IgY(SIL)}}}{A_{\text{IgY(WSPF)}}} \times 100 \quad (4)$$

where,  $A_{\text{IgY(SIL)}}$  corresponds to the peak area of IgY adsorbed on the SIL, and  $A_{\text{IgY(WSPF)}}$  corresponds to the peak area of IgY in the initial biological media (WSPF).

#### Assessment of SIL materials for IgY purification from WSPF

A preliminary screening was conducted with [Ssi][C<sub>3</sub>mim]Cl, [Ssi][N<sub>3444</sub>]Cl, and [Ssi][N<sub>3888</sub>]Cl, according to the protocol described by Capela *et al.*,<sup>10</sup> to evaluate their ability to purify IgY from the WSPF. For comparison purposes, the activated spherical silica was employed as a control. Each material was placed in 1.5 mL microtubes, according to the following operating conditions: Solid: Liquid (S:L) ratio of 100 mg mL<sup>-1</sup>, which consisted on putting 50 mg of the material in contact with 500 µL of WSPF in an appropriate buffer, according to the selected pH; pH of 3.0, 5.0, 7.0, and 9.0, and a contact time of 60 min. The samples were stirred on a programmable rotator-mixer PTR-30 Grant-bio, followed by their centrifugation for 20 min at 13000 rpm in a VRW MICRO STAR 17 to separate the aqueous solution from the material, that remained in the bottom of the microtube. All aqueous solutions were analyzed by SE-HPLC, being diluted at a 1:1 (v:v) ratio with the mobile phase.

#### Optimization of the purification process by response surface methodology

Following the initial screening, a factorial design was employed to optimize the IgY recovery yield and purification. Therefore, a 2<sup>3</sup> factorial design was accomplished to optimize three independent variables, *i.e.*, the S:L ratio (mg of material per mL of aqueous solution of biological media), pH and contact time (min), both for the maximization of IgY purity and recovery yield. The experimental data was processed based on the Eqns S1–S3, outlined in the Supporting Information. The variables were studied at the central point (zero level), factorial points (1 and -1, level one), and axial points (level  $\alpha$ ), with the planning of the 2<sup>3</sup> factorial design, depicted in Table S1 of the Supporting Information. According to Eqns S2 and S3, provided in the Supporting Information, 20 experiments were conducted, and a value of 1.68 was adopted, respectively. The range was defined based on preliminary results, and the central point was set at S:L ratio of 100 mg mL<sup>-1</sup>, pH 3.0, 5.0, 7.0, and 9.0, and 60 min of contact. The range of experiments, underwent with the coded and uncoded coefficients, is presented in Table S2 of the Supporting Information. The results obtained were statistically analyzed by resorting to STATISTICA<sup>TM</sup> software, with a 95% confidence level. Three-dimensional surface response plots were carried out by modifying two variables within the

experimental range and preserving the other factors at the central point, being the contour plots and response surfaces designed in STATISTICA<sup>TM</sup> software.

## RESULTS AND DISCUSSION

### Characterization of the supported ionic liquids (SILs)

In this work, three SILs, namely [Ssi][C<sub>3</sub>mim]Cl, [Ssi][N<sub>3888</sub>]Cl, and [Ssi][N<sub>3444</sub>]Cl, were synthesized in a single step (Fig. 1). Their carbon, hydrogen, and nitrogen contents were determined by elemental analysis, and their respective BA was calculated, considering a S<sub>BET</sub> for the spherical silica of 288.59 m<sup>2</sup> g<sup>-1</sup>. The zeta potential curves as a function of pH, which are presented in Fig. S1 of the Supporting Information, were also prepared and employed to determine the PZC of the activated spherical silica and the SILs. The results obtained for these three parameters are provided in Table 1.

In all SILs, the presence of carbon (C), hydrogen (H), and nitrogen (N) was confirmed, suggesting a successful functionalization, with the ILs covalently bond to the surface of spherical silica, which inherently lacks these elements. Contrarily to [Ssi][C<sub>3</sub>mim]Cl, which exhibited the highest nitrogen content of 2.538%, [Ssi][N<sub>3444</sub>]Cl and [Ssi][N<sub>3888</sub>]Cl presented lower amounts, of 0.096 and 0.085%, respectively, suggesting a more modest degree of functionalization. It is important to highlight that there is no proportional relationship between the BA and the molar amount of the cation source, being in agreement with the literature.<sup>10</sup> Therefore, even when the same volume of the amine solution was used to synthesize the SILs, different degrees of functionalization can be observed, which can be justified by the stereochemical effect.<sup>13,26</sup> Accordingly, even though the same molarity of the cation source was employed in the preparation of [Ssi][C<sub>3</sub>mim]Cl, [Ssi][N<sub>3444</sub>]Cl, and [Ssi][N<sub>3888</sub>]Cl, different degrees of functionalization were obtained.

The PZC values for the activated spherical silica and SILs were determined based on the graphical representations of zeta potential as a function of pH (Fig. S1 of the Supporting Information). The first material exhibited the lowest PZC value of 3.2, whereas [Ssi][C<sub>3</sub>mim]Cl, [Ssi][N<sub>3444</sub>]Cl, and [Ssi][N<sub>3888</sub>]Cl, presented higher values for this parameter, of 10.1, 5.2, and 5.6, respectively, indicating that their surfaces are more positively charged (Table 1). This is due to the grafting of the IL cations onto the spherical silica surface, confirming the successful functionalization of silica with ILs.

<sup>13</sup>C NMR was also used to characterize the SILs and confirm their successful preparation, being the resultant spectra depicted in Fig. 2.

Regarding [Ssi][N<sub>3444</sub>]Cl and [Ssi][N<sub>3888</sub>]Cl, three peaks at 10, 27, and 46 ppm were identified, corresponding to the three carbons

**Table 1.** Chemical amount (n(mol)) of the cation source used in the synthesis, weight percentages of carbon (%C), hydrogen (%H), and nitrogen (%N) determined by elemental analysis (EA); BA (µmol m<sup>-2</sup>), and PZC of the activated silica and all synthesized SILs, *i.e.*, [Ssi][C<sub>3</sub>mim]Cl, [Ssi][N<sub>3444</sub>]Cl, and [Ssi][N<sub>3888</sub>]Cl

SILs	n (mol)	EA			BA (µmol m <sup>-2</sup> )	PZC
		C (%)	H (%)	N (%)		
Activated spherical silica	—	—	—	—	—	3.2
[Ssi][C <sub>3</sub> mim]Cl	0.035	8.816	1.684	2.538	3.14	10.1
[Ssi][N <sub>3444</sub> ]Cl	0.035	6.661	1.205	0.096	0.23	5.2
[Ssi][N <sub>3888</sub> ]Cl	0.035	6.687	1.435	0.085	0.21	5.6

of the propyl alkyl chain. The NMR spectra of the previous SILs resemble those of the intermediate material ([Si][C<sub>3</sub>]Cl) used in the two-step SIL synthesis previously reported our research group.<sup>10,25</sup> This similarity can be attributed to the low degree of functionalization presented by [Ssi][N<sub>3444</sub>]Cl and [Ssi][N<sub>3888</sub>]Cl, which is in accordance with the elemental analysis results (Table 1). Six peaks were identified for [Ssi][C<sub>3</sub>mim]Cl, namely at 10, 25, and 37 ppm, corresponding to the three carbon atoms of the alkyl side chain of the aromatic ring (C2, C1, and C6), respectively. The aromatic carbons of the imidazolium ring (C5 and C4) are represented by the signals that range from 122 to 137 ppm, respectively. Moreover, the peak identified at 52 ppm is associated with the last carbon (C3) of the alkyl chain, confirming the silica functionalization.

ATR-FTIR was further used to confirm the silica functionalization, being the spectra for the activated spherical silica and the three synthesized SILs depicted in Fig. 3. The gathered results are in accordance with the ones demonstrated by Capela *et al.*,<sup>10</sup> where a band corresponding to the Si-OH stretching, which corresponds to the initial stage of the reaction of the activated spherical silica

with the 3-chloropropyltrimethoxysilane, is found at approximately 3400–3900 cm<sup>-1</sup>.

The aliphatic chain C–N from all the SILs following their reaction with the respective cation source is represented by the band at 1100 cm<sup>-1</sup>, while the comparatively weaker bands at 2900–3200 cm<sup>-1</sup> correspond to the stretching vibrations of CH<sub>3</sub> and CH<sub>2</sub>. Moreover, the peaks at 400–900 cm<sup>-1</sup> are associated with the chloride anion from the first reaction, as well as with the OH bending from the initial interaction of the activated silica with the anion.

The chemical characterization of the synthesized SILs by elemental analysis, zeta potential measurements, CPMAS <sup>13</sup>C NMR, and ATR-FTIR, confirm their successful functionalization. This evidence is in agreement with the literature,<sup>10</sup> in which SILs were synthesized by functionalizing a 60 Å silica with the same ILs; however, through a two-step process. In this work, a similar functionalization was accomplished in a single step, leading to a reduction of both organic solvent's usage and experimental time, while maintaining the same degree of silica functionalization.

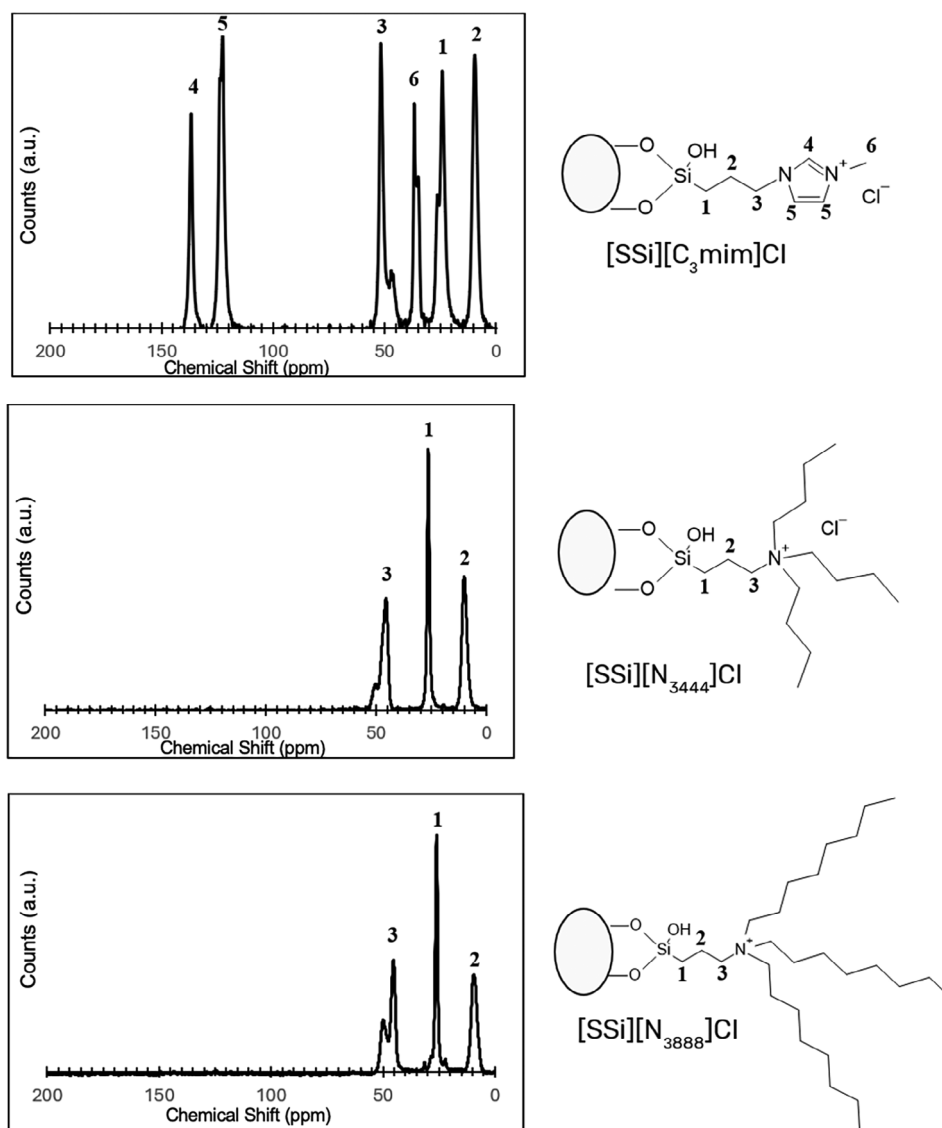


**Figure 2.** Solid-state <sup>13</sup>C NMR spectra of [Ssi][C<sub>3</sub>mim]Cl, [Ssi][N<sub>3444</sub>]Cl, and [Ssi][N<sub>3888</sub>]Cl.

### IgY quantification

The WSPF was analyzed by SE-HPLC to quantify the contents of the main proteins present, *i.e.*, IgY,  $\alpha$ , and  $\beta$ -livetins. A comparison of the conventional chromatograms for pure IgY and WSPF is depicted in Fig. 4.

There is a single and defined peak at the retention time of 13.3 min, corresponding to IgY, when dealing with the pure IgY fraction. On the other hand, the WSPF chromatogram reveals the presence of two additional peaks, at the retention time of 15 and 16 min, corresponding to other major WSPF proteins, *i.e.*,  $\alpha$  and  $\beta$  livetins, respectively. This evidence is in accordance with their respective molecular weights of 180, 80 and 45 kDa for IgY,  $\alpha$  and  $\beta$ -livetins, respectively.<sup>28,29</sup>

### Assessment of SIL materials for IgY purification from the WSPF

An initial assessment of the interaction between the proteins presented in the WSPF (IgY,  $\alpha$  and  $\beta$ -livetins) and the SILs and activated spherical silica was carried out. All materials were subjected to the same operating conditions, which included a S:L ratio of 100 mg mL<sup>-1</sup>, a contact time of 60 min, and pH values of 3.0, 5.0, 7.0 and 9.0. All samples were analyzed by SE-HPLC, being the respective chromatograms depicted in Fig. 5.

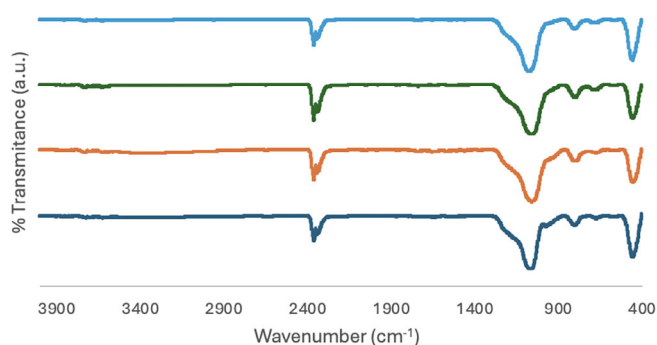


**Figure 3.** ATR-FTIR spectra of [Ssi][N<sub>3888</sub>]Cl (light blue), [Ssi][N<sub>3444</sub>]Cl (green), [Ssi][C<sub>3</sub>mim]Cl (orange) and activated spherical silica (dark blue).

This study was crucial to understanding the behavior of SILs after contact with a complex biological matrix, *i.e.*, WSPF, and to unveil how the modification of the medium pH affects protein adsorption. As can be seen in Fig. 5, the chromatograms of the WSPF before and after the contact with the activated spherical silica (non-IL modified) are similar, demonstrating that the adsorbent material exhibits no selectivity for any of the proteins in all pH range studied. On the other hand, a decrease in the peaks intensity of the proteins present in the WSPF is seen after contact with SILs at pH values ranging from 3.0 to 7.0. In fact, the highest decrease on peaks intensity was obtained after contact with [Ssi][C<sub>3</sub>mim]Cl, at pH 3.0 and 5.0. Additionally, at pH 9.0, no protein adsorption was found for any of the SILs under study. Accordingly, it is possible to hypothesize that this pH environment may have resulted in protein aggregation and therefore, less adsorption.

The adsorption profiles of both [Ssi][N<sub>3444</sub>]Cl and [Ssi][N<sub>3888</sub>]Cl are similar at pH 3.0, 5.0, and 7.0, indicating that other intermolecular forces contributed more significantly to adsorption than electrostatic interactions. Therefore, van der Waals interactions with the alkyl chains of the SILs might be dominant, giving place to the hydrophobic effect. A slight increase of adsorption was observed at pH 7.0, which might result from electrostatic interactions among the charged proteins and SILs. This phenomenon could be a result of the negative charge of the proteins in a less acidic environment (IgY,  $\alpha$ , and  $\beta$ -livetins isoelectric points (*pI*) correspond to 5.7, 4.7, and 5.6, respectively).<sup>28,29</sup> The effect is stronger for [Ssi][N<sub>3444</sub>]Cl, which presents shorter alkyl chains attached to the quaternary nitrogen. Even considering the hydrophobic interaction as the predominant effect, it was expected that adsorption onto the SILs would increase above the *pI* of the proteins, due to electrostatic interactions with the quaternary ammonium group. However, this behavior was not observed for [Ssi][C<sub>3</sub>mim]Cl. The adsorption onto the latter material was stronger at pH 3.0 and 5.0, reinforcing that electrostatic interactions are probably not the dominant ones for all SILs. It is possible to attribute the stronger interaction of the proteins present in the WSPF with [Ssi][C<sub>3</sub>mim]Cl to hydrogen bonding and  $\pi$ - $\pi$  interactions. The hydrogen atoms on the imidazole ring, particularly in the C2-H, can establish hydrogen bonds with oxygen atoms at the protein surface; on the other hand, the quaternary

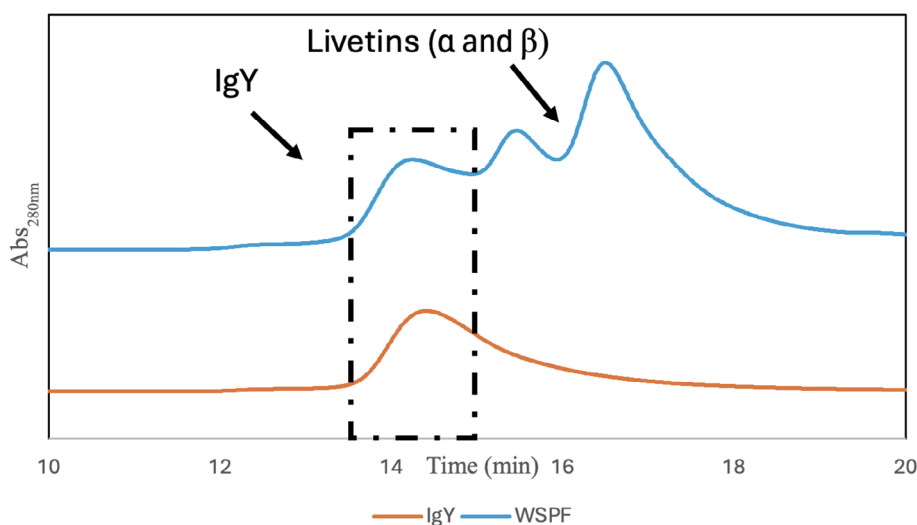


**Figure 4.** SE-HPLC chromatograms of pure IgY (orange) and WSPF (light blue), accompanied by the identification of their major proteins.

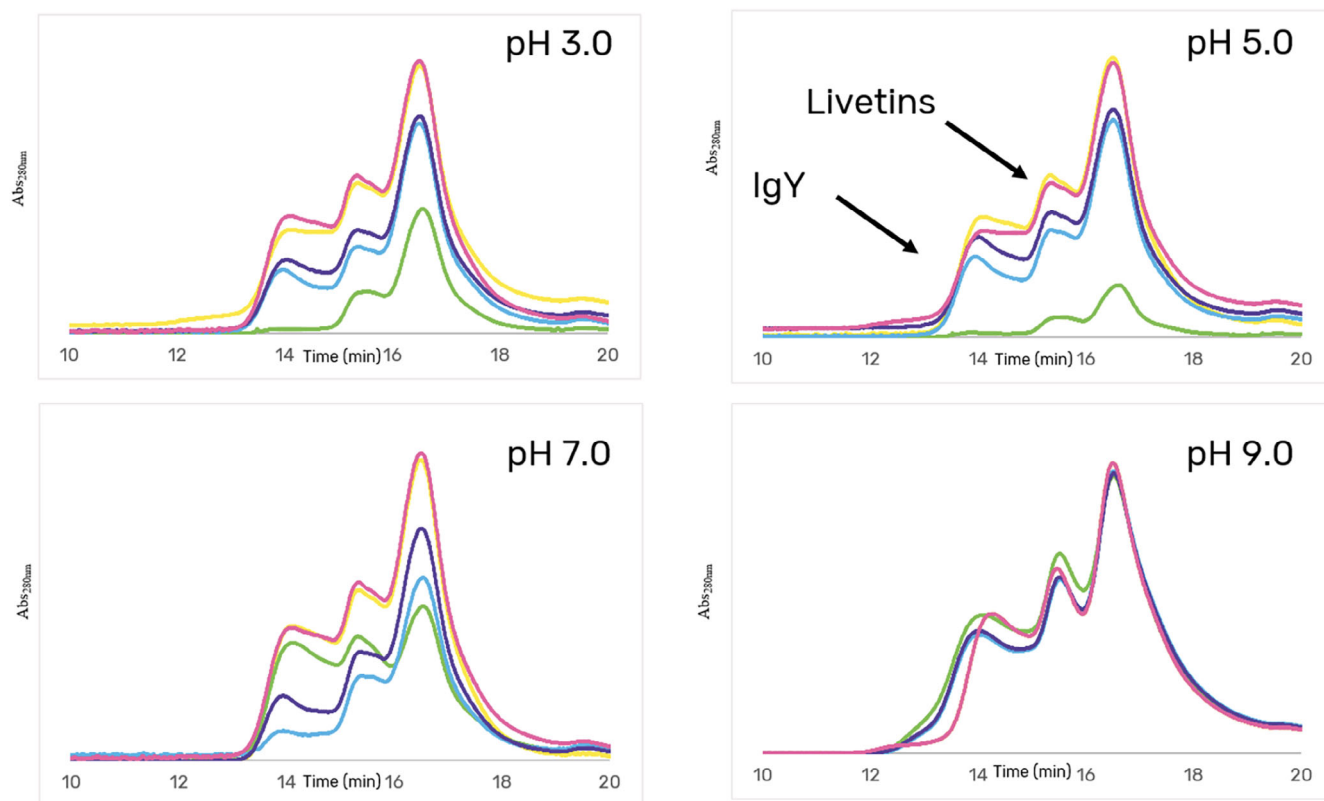


**Figure 5.** SE-HPLC chromatograms of WSPF at pH 3.0, 5.0, 7.0 and 9.0 before (yellow) and after the contact with the activated spherical silica (pink), [Ssi][C<sub>3</sub>mim]Cl (green), [Ssi][N<sub>3444</sub>]Cl (blue), and [Ssi][N<sub>3888</sub>]Cl (purple).

ammonium cations present in [Ssi][N<sub>3444</sub>]Cl and [Ssi][N<sub>3888</sub>]Cl cannot act as hydrogen bond donors or acceptors.<sup>30</sup> Also, the imidazole ring can perform  $\pi$ - $\pi$  interactions with proteins, and the substitutions in both nitrogens of the imidazole ring of [Ssi][C<sub>3</sub>mim]Cl enhance the  $\pi$ -electron density, potentially making the  $\pi$ - $\pi$  interactions stronger.<sup>31</sup> Finally, it is also important to consider that its high degree of functionalization may also contribute to the stronger binding.

In a computational study, the crystalline structure of the Fc region of IgY was employed to investigate interactions and binding sites with ILs during aqueous two-phase-based purification.<sup>32</sup> It was possible to conclude that the process was primarily driven by hydrogen bonding and van der Waals interactions. In another study, Shu *et al.*<sup>33</sup> conducted combined experimental and computational studies to investigate the interactions between hydrophilic proteins, such as Bovine Serum Albumin (BSA) and imidazolium-based ILs. Their findings indicated that hydrophobic and electrostatic interactions were the ones to predominate. Tong *et al.*<sup>34</sup> employed Hydrophobic Charge-Induction Chromatography (HCIC) to purify the Fc fraction of goose IgY, resorting to a 2-mercapto-1-methyl-imidazole (MMI) ligand coupled to an agarose matrix, used to prepare the HCIC gel. The authors<sup>34</sup> demonstrated that IgY( $\Delta$ Fc) binding to the MMI-functionalized agarose was dominated by hydrophobic and thiophilic interactions.

### Purification process optimization

The influence of several parameters, namely the S:L ratio, pH, and contact time on IgY purification was investigated by determining its purity and recovery yield percentages, forecasting the

optimization of the process. Accordingly, two main paradigms could be anticipated when envisioning IgY purification from WSPF: (1) the antibody is adsorbed onto the SIL, leaving  $\alpha$  and  $\beta$ -livetins in solution, or (2) the latter proteins are adsorbed onto the material, leaving IgY in solution. The best results were achieved with the first approach. The optimal IgY purification conditions, in terms of contact time, pH, and S:L ratio, for each SIL are summarized in Table 2.

The response surface and respective contour plots for IgY purity and recovery yield are depicted in Figs 6 and 7, respectively. The quantitative results, the statistical analysis, as well as comparative tables of experimental and theoretical purity and recovery yield are provided in Tables S3–S21 in the Supporting Information.

[Ssi][C<sub>3</sub>mim]Cl was able to adsorb IgY with a purity and a recovery yield of 90.1 and 20.2%, respectively, when it was placed in contact for 30 min with the WSPF at pH 3.0 and S:L ratio of 100 mg mL<sup>-1</sup> (Table 2). As can be seen in Fig. 6(A), (B), the optimal conditions for purity are located near the optimal zone (dark red), that includes pH values ranging from 4 to 6, and S:L ratio of 50 to 80 mg mL<sup>-1</sup>. Moreover, according to Fig. 7(A), (B), a similar behavior was observed for IgY recovery yield, with optimal conditions located in the optimal zone (dark red) that includes pH values from 4 to 5, and S:L ratio of 60–80 mg mL<sup>-1</sup>. Notwithstanding, the best recovery yield for IgY, obtained by [Ssi][C<sub>3</sub>mim]Cl, was achieved at lower pH (5.0), S:L ratio (65 mg mL<sup>-1</sup>), and contact time (9.54 min). From the Pareto chart, depicted in Fig. S2 A in the Supporting Information, the contact time factor was significant for the IgY purity, whereas for the recovery yield, none of the studied factors demonstrated a significant impact (Fig. S3(A) in the Supporting Information).

**Table 2.** Optimal conditions and results for IgY purification using SILs

SIL	Conditions			Results	
	Contact time (min)	pH	S:L ratio (mg mL <sup>-1</sup> )	%Purity	%Recovery yield
[Ssi][C <sub>3</sub> mim]Cl	30	3	100	90.1	20.2
[Ssi][N <sub>3444</sub> ]Cl	60	5	65	81.1	14.5
[Ssi][N <sub>3888</sub> ]Cl	30	3	100	89.4	23.7

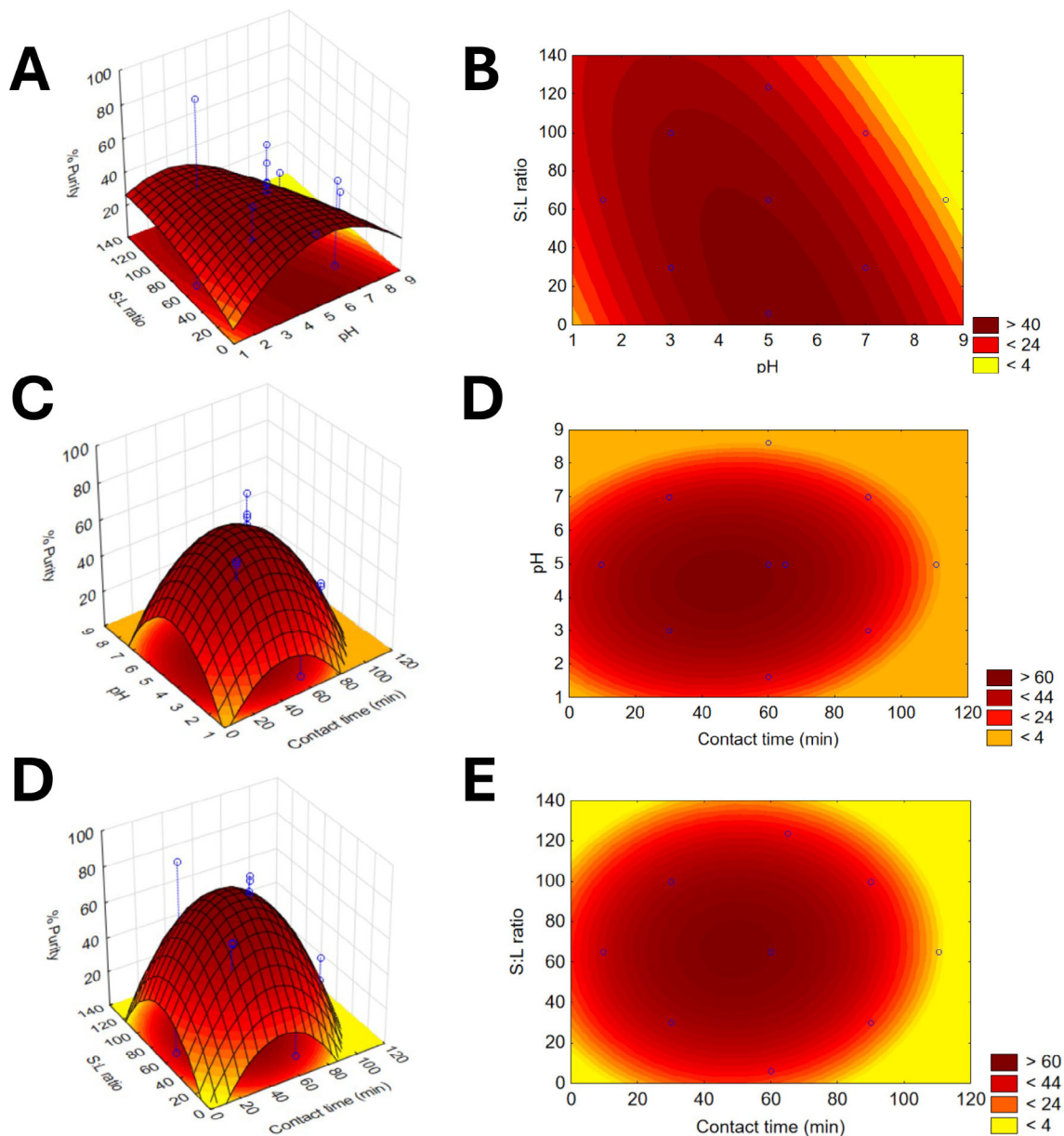


**Figure 6.** Response surface plots (left) and contour plots (right) for IgY % Purity using: (A) and (B) [Ssi][C<sub>3</sub>mim]Cl (with emphasis on S:L ratio of 65 mg mL<sup>-1</sup>); (C) and (D) [Ssi][N<sub>3444</sub>]Cl (with emphasis on S:L ratio of 65 mg mL<sup>-1</sup>); and (E) and (F) [Ssi][N<sub>3888</sub>]Cl (with emphasis on pH 5.0).

On the other hand, [Ssi][N<sub>3444</sub>]Cl was able to adsorb IgY with a purity and a recovery yield of 81.1 and 14.5%, respectively, after being placed in contact with the WSPF for 60 min, at pH 5.0 and a S:L ratio of 65 mg mL<sup>-1</sup> (Table 2). According to Fig. 6(C), (D), it is evident that the optimal conditions for purity are in the pH

range of 3 to 5, and a contact time of 30–70 min, being in accordance with the ones settled experimentally. As can be seen in Figs. 7 C and D, the optimal conditions for IgY recovery yield are in the optimal zone (dark red) that comprises a pH range of 4 to 5, and a S:L ratio of 50–70 mg mL<sup>-1</sup>. Despite the experimental

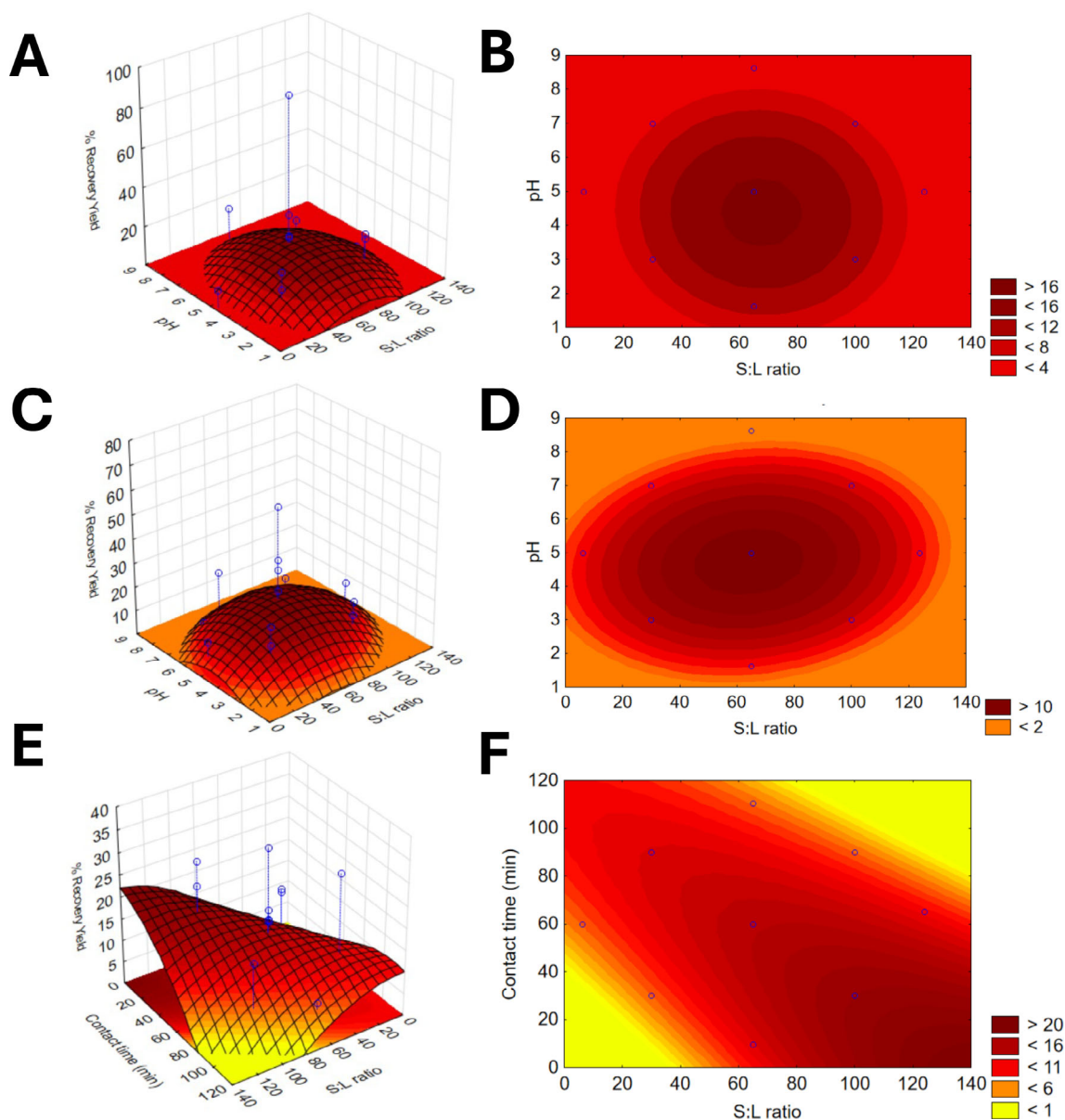


**Figure 7.** Response surface plots (left) and contour plots (right) for IgY % Recovery yield using (A) and (B)  $[\text{Ssi}][\text{C}_3\text{mim}]\text{Cl}$ ; (C) and (D)  $[\text{Ssi}][\text{N}_{3444}]\text{Cl}$ ; and (E) and (F)  $[\text{Ssi}][\text{N}_{3888}]\text{Cl}$ .

optimal conditions for  $[\text{Ssi}][\text{N}_{3444}]\text{Cl}$  being set at pH 5.0, a S:L ratio of  $65 \text{ mg mL}^{-1}$  and a contact time of 60 min, the best recovery yield for the antibody of interest (35.14%) was achieved for a higher contact time, of 110.45 min. From the Pareto chart, depicted in Fig. S2 B in the Supporting Information, it is possible to conclude that the quadratic functions of contact time and pH had a significant influence on this response.

Finally,  $[\text{Ssi}][\text{N}_{3888}]\text{Cl}$  was able to adsorb IgY with a purity and recovery yield of 89.4 and 23.7%, respectively, after being placed in contact with the WSPF for 30 min, at pH 3.0, and an S:L ratio of  $100 \text{ mg mL}^{-1}$  (Table 2). From Fig. 6(E), (F), it is evident that the optimal conditions regarding purity include an S:L ratio ranging between 40 and  $100 \text{ mg mL}^{-1}$ , and a contact time of 30–70 min, which is in accordance with the ones defined experimentally. Regarding Fig. 7(E), (F), it is evident that the optimal conditions

for recovery yield are in an S:L ratio of 70–80  $\text{mg mL}^{-1}$  and a contact time of 40–60 min, which are different of the ones settled experimentally. It is also important to reinforce that the best recovery yield for IgY obtained by  $[\text{Ssi}][\text{N}_{3888}]\text{Cl}$  (33.96%) was achieved at higher pH values and contact times (pH 5.0 and 60 min) and lower S:L ratio ( $65 \text{ mg mL}^{-1}$ ). Despite the *P*-values observed, the statistical analysis, presented in the Supporting Information, clearly indicates the contact time as the variable that most influence the IgY purity. Overall, the most promising conditions for the purity and recovery yield of IgY from WSPF can be clearly identified, despite some differences between the predicted and experimental values of the three variables in study for  $[\text{Ssi}][\text{C}_3\text{mim}]\text{Cl}$ ,  $[\text{Ssi}][\text{N}_{3444}]\text{Cl}$ , and  $[\text{Ssi}][\text{N}_{3888}]\text{Cl}$  are seen, as can be appraised in Tables S4 and S7, S10 and S13, and S16 and S19, in the Supporting Information, respectively.

It is evident that the [Ssi][C<sub>3</sub>min]Cl demonstrated to be the material that can absorb the antibody of interest with the highest purity level (90.1%), proving to be a promising option to be further studied as a stationary phase in preparative liquid chromatography. Several advantages associated with the use of SILs for protein purification can be pointed out. For instance, the immobilization of an IL allows for taking advantage of many IL properties, being the most relevant in this work the ability to fine-tune the ligand chemical structure, and as such, the affinity towards the target biomolecule.

In addition to the purification of IgY, SILs have shown to be promising in other target separations. In the work developed by Neves *et al.*,<sup>35</sup> a macroporous chromatographic support functionalized with an IL was used for nucleic acid purification, demonstrating effective regeneration and reuse without compromising the separation performance. Similarly, Almeida *et al.*<sup>18</sup> applied SILs for the removal of anti-inflammatory compounds from aqueous media, using systems that were regenerated and reused with no significant loss in recovery efficiency. Additionally, several regeneration and recovery techniques for ILs are already in practice, including distillation, liquid–liquid extraction with Aqueous Biphasic Systems, membrane technology, and adsorption.<sup>36</sup>

In an industry context, scalability is also a critical factor. For instance, Hycapure-Hg is commercially available as an IL incorporating the chlorocuprate anion, dispersed within high-surface-area porous solid matrices, and has maintained low mercury concentrations at the plant outlet after three years of continuous operation. The progress in designing larger and more advanced flow reactors has significantly enhanced the scalability of SIL systems for industrial applications.<sup>37,38</sup> Collectively, these findings underscore the potential of SILs, which combine scalability with the possibility of regeneration and reuse.

## CONCLUSION

This work demonstrated the potential of SILs as selective materials for the purification of immunoglobulin Y (IgY) from a complex biological matrix, *i.e.* the WSPF. Three SILs were synthesized in a single step and optimized using statistical design, achieving purity values of up to 90%, and recovery yields of up to 20%, under mild conditions. The materials showed different interaction IgY, enabling strategic tuning of purification performance. The process reduced solvent consumption and reaction time, aligning with green chemistry principles. These results highlight the feasibility of SIL-based platforms for industrial-scale antibody purification, offering a scalable, environmentally responsible alternative to traditional downstream processing.

## ACKNOWLEDGEMENTS

This work was developed within the scope of the project CICECO-Aveiro Institute of Materials, UIDB/50011/2020 (DOI 10.54499/UIDB/50011/2020), UIDP/50011/2020 (DOI 10.54499/UIDP/50011/2020) & LA/P/0006/2020 (DOI 10.54499/LA/P/0006/2020) financed by national funds through the FCT/MCTES (PID-DAC). CA acknowledges FCT for the doctoral grant 2022.11570. BD. MCN acknowledges FCT for the research contract CEECIND/00383/2017/CP1459/CT0031 (DOI 10.54499/CEECIND/00383/2017/CP1459/CT0031). We also acknowledge grants from the National Council for Scientific and Technological Development (CNPq-Brazil, process number: 309953/2020-0) and the Coordination of Improvement of Higher Education Personnel (CAPES-

Brazil, finance code: 001). Open access publication funding provided by FCT (b-on).

## DATA AVAILABILITY STATEMENT

Data will be available from the authors upon request.

## CONFLICT OF INTEREST

The authors declare that there are no known competing financial interests or personal relationships that could interfere with the work reported on this paper.

## AUTHOR CONTRIBUTIONS

**Amanda R. P. Silva:** investigation, writing-the original draft. **Catarina Almeida:** investigation, writing-the original draft. **Márcia C. Neves:** conceptualization; writing-review and editing, visualization, supervision. **Carlota O. Rangel-Yagui:** conceptualization; writing-review and editing, visualization, supervision, project administration, funding acquisition. **Mara G. Freire:** conceptualization; writing-review and editing, visualization, supervision, project administration, funding acquisition.

## SUPPORTING INFORMATION

Supporting information may be found in the online version of this article.

## REFERENCES

- Megha KB and Mohanan PV, Role of immunoglobulin and antibodies in disease management. *Int J Biol Macromol* **169**:28–38 (2021).
- Spillner E, Braren I, Greunke K, Seismann H, Blank S and du Plessis D, Avian IgY antibodies and their recombinant equivalents in research, diagnostics and therapy. *Biologicals* **40**:313–322 (2012).
- Schade R, Calzado EG, Sarmiento R, Chacana PA, Porankiewicz-Asplund J and Terzolo HR, Chicken egg yolk antibodies (IgY-technology): a review of progress in production and use in research and human and veterinary medicine. *Altern Lab Anim* **33**: 129–154 (2005).
- Yakhkeshi S, Wu R, Chelliappan B and Zhang X, Trends in industrialization and commercialization of IgY technology. *Front Immunol* **13**: 991931 (2022).
- Wu R, Yakhkeshi S and Zhang X, Scientometric analysis and perspective of IgY technology study. *Poult Sci* **101**:101713 (2022).
- Hernández-Campos FJ, Brito-De La Fuente E and Torrestiana-SÁNCHEZ B, Purification of egg yolk immunoglobulin (IgY) by ultrafiltration: effect of pH, ionic strength, and membrane properties. *J Agric Food Chem* **58**:187–193 (2010).
- Rahman S, Van Nguyen S, Icatlo FC, Umeda K and Kodama Y, Oral passive IgY-based immunotherapeutics. *Hum Vaccin Immunother* **9**: 1039–1048 (2013).
- Ge S, Yang Y, Chelliappan B, Michael A, Zhong F and Zhang X, Evaluation of different IgY preparation methods and storage stability as potential animal feed supplement. *Pak J Zool* **52**:2305–2311 (2020).
- Campisciano V, Giacalone F and Gruttadauria M, Supported ionic liquids: A versatile and useful class of materials. *Chem Rec* **17**:918–938 (2017).
- Capela EV, Bairos J, Pedro AQ, Neves MC, Raquel Aires-Barros M, Azevedo AM *et al.*, Supported ionic liquids as customizable materials to purify immunoglobulin G. *Sep Purif Technol* **305**:122464 (2023).
- Earle MJ, Esperança JMSS, Gilea MA, Lopes JNC, Rebelo LPN, Magee JW *et al.*, The distillation and volatility of ionic liquids. *Nature* **439**:831–834 (2006).
- Ventura SPM, E Silva FA, Quental MV, Mondal D, Freire MG and Coutinho JAP, Ionic-liquid-mediated extraction and separation processes for bioactive compounds: past, present, and future trends. *Chem Rev* **117**:6984–7052 (2017).

- 13 Nunes JCF, Almeida MR, Bento RMF, Pereira MM, Santos-Ebinuma VC, Neves MC *et al.*, Enhanced enzyme reuse through the bioconjugation of L-asparaginase and silica-based supported ionic liquid-like phase materials. *Molecules* **27**:929 (2022).
- 14 Qiu H, Jiang S, Liu X and Zhao L, Novel imidazolium stationary phase for high-performance liquid chromatography. *J Chromatogr A* **1116**:46–50 (2006).
- 15 Fontanals N, Borrull F and Marcé RM, Ionic liquids in solid-phase extraction. *TrAC Trends Anal Chem* **41**:15–26 (2012).
- 16 Wang Q, Baker GA, Baker SN and Colón LA, Surface confined ionic liquid as a stationary phase for HPLC. *Analyst* **131**:1000–1005 (2006).
- 17 Van Roosendaal S, Regadío M, Roosen J and Binnemans K, Selective recovery of indium from iron-rich solutions using an Aliquat 336 iodide supported ionic liquid phase (SILP). *Sep Purif Technol* **212**:843–853 (2019).
- 18 Almeida HFD, Neves MC, Trindade T, Marrucho IM and Freire MG, Supported ionic liquids as efficient materials to remove non-steroidal anti-inflammatory drugs from aqueous media. *Chem Eng J* **381**:122616 (2020).
- 19 Van de Voorde M, Van Hecke K, Binnemans K and Cardinaels T, Supported ionic liquid phases for the separation of samarium and europium in nitrate media: towards purification of medical samarium-153. *Sep Purif Technol* **232**:115939 (2020).
- 20 Song H, Yang C, Yohannes A and Yao S, Acidic ionic liquid modified silica gel for adsorption and separation of bovine serum albumin (BSA). *RSC Adv* **6**:107452–107462 (2016).
- 21 Zhao G, Chen S, Chen XW and He RH, Selective isolation of hemoglobin by use of imidazolium-modified polystyrene as extractant. *Anal Bioanal Chem* **405**:5353–5358 (2013).
- 22 Shu Y, Chen XW and Wang JH, Ionic liquid–polyvinyl chloride ionomer for highly selective isolation of basic proteins. *Talanta* **8**:637–642 (2010).
- 23 Almeida MR, Nunes JCF, Pereira MM, Bento HBS, Pedrolli DB, Santos-Ebinuma VC *et al.*, Supported ionic liquids to purify microbial L-asparaginase. *Biochem Eng J* **211**:109445 (2024).
- 24 Qiu H, Jiang S and Liu X, N-methylimidazolium anion-exchange stationary phase for high-performance liquid chromatography. *J Chromatogr A* **1103**:265–270 (2006).
- 25 Bernardo SC, Araújo BR, Sousa ACA, Barros RA, Cristovão AC, Neves MC *et al.*, Supported ionic liquids for the efficient removal of acetylsalicylic acid from aqueous solutions. *Eur J Inorg Chem* **2020**:2380–2389 (2020).
- 26 Nunes JCF, Almeida MR, de Paiva GB, Pedrolli DB, Santos-Ebinuma VC, Neves MC *et al.*, A flow-through strategy using supported ionic liquids for L-asparaginase purification. *Sep Purif Technol* **315**:123718 (2023).
- 27 Liu J, Yang J, Xu H, Lu J and Cui Z, A new membrane based process to isolate immunoglobulin from chicken egg yolk. *Food Chem* **122**:747–752 (2010).
- 28 Almeida MR, Ferreira F, Domingues P, A. P. Coutinho J and Freire MG, Towards the purification of IgY from egg yolk by centrifugal partition chromatography. *Sep Purif Technol* **299**:121697 (2022).
- 29 Zambrowicz A, Dąbrowska A, Bobak Ł and Szołtysik M, Egg yolk proteins and peptides with biological activity. *Postepy Hig Med Dosw (Online)* **68**:1524–1529 (2014).
- 30 Reddy P and Letcher TM, Phase equilibrium studies on ionic liquid systems for industrial separation processes of complex organic mixtures, in *Thermodynamics, Solubility and Environmental Issues*, Elsevier, Amsterdam, Netherlands, pp. 85–111 (2007).
- 31 Matthews RP, Welton T and Hunt PA, Competitive pi interactions and hydrogen bonding within imidazolium ionic liquids. *Phys Chem Chem Phys* **16**:3238–3253 (2014).
- 32 Taha M, Almeida MR, E Silva FA, Domingues P, Ventura SPM, Coutinho JAP *et al.*, Novel biocompatible and self-buffering ionic liquids for biopharmaceutical applications. *Chemistry* **21**:4781–4788 (2015).
- 33 Shu Y, Liu M, Chen S, Chen X and Wang J, New insight into molecular interactions of imidazolium ionic liquids with bovine serum albumin. *J Phys Chem B* **115**:12306–12314 (2011).
- 34 Tong HF, Lin DQ, Pan Y and Yao SJ, A new purification process for goose immunoglobulin IgY( $\Delta$ Fc) with hydrophobic charge-induction chromatography. *Biochem Eng J* **56**:205–211 (2011).
- 35 Neves MC, Pereira P, Pedro AQ, Martins JC, Trindade T, Queiroz JA *et al.*, Improved ionic-liquid-functionalized macroporous supports able to purify nucleic acids in one step. *Mater Today Biol* **8**:100086 (2020).
- 36 Khoo YS, Tjong TC, Chew JW and Hu X, Techniques for recovery and recycling of ionic liquids: A review. *Sci Total Environ* **922**:171238 (2024).
- 37 Villa R, Alvarez E, Porcar R, Garcia-Verdugo E, Luis SV and Lozano P, Ionic liquids as an enabling tool to integrate reaction and separation processes. *Green Chem* **21**:6527–6544 (2019).
- 38 Wolny A and Chrobok A, Silica-based supported ionic liquid-like phases as heterogeneous catalysts. *Molecules* **27**:5900 (2022).